Published in final edited form as:
Chem Sci. 2013 September 1; 4(9): 3447–3454. doi:10.1039/C3SC50726B.

DNA strands with alternating incorporations of LNA and 2'-*O*-(pyren-1-yl)methyluridine: SNP-discriminating RNA detection probes†

Saswata Karmakar and **Patrick J. Hrdlicka***
University of Idaho, Department of Chemistry, Moscow, ID 83844-2343, USA

Abstract

Detection of nucleic acids using fluorophore-modified oligonucleotides forms the basis of many important applications in molecular biology, genetics and medical diagnostics. Here we demonstrate that DNA strands with central segments of alternating locked nucleic acid (LNA) and 2'-*O*-(pyren-1-yl)methyluridine monomers display very large and highly mismatch-sensitive increases in fluorescence emission upon RNA hybridization, whereas corresponding "LNA-free" controls do not. Absorbance spectra strongly suggest that LNA-induced conformational tuning of flanking 2'-*O*-(pyren-1-yl)methyluridine monomers places the reporter group in the minor groove upon RNA binding, whereby pyrene-nucleobase interactions leading to quenching of fluorescence are minimized. Accordingly, these easy-to-synthesize probes are promising SNP-discriminating RNA detection probes.

Introduction

Detection of nucleic acids using homogenous assays involving fluorophore-modified oligonucleotides forms the basis of many important applications in molecular biology, genetics and medical diagnostics[1,2] including detection of microorganisms,[3] real-time PCR monitoring,[4] detection of single nucleotide polymorphisms (SNPs),[5] fluorescence in situ hybridization (FISH),[6] and in vivo RNA imaging.[7,8] Pyrene-modified oligonucleotides have been studied extensively as model systems[9,10] due to the high quantum yield and position-dependent emission characteristics of pyrene.[9–12] Thus, localization of pyrene moieties in one of the duplex grooves typically results in: i) strong fluorescence in the 370–420 nm 'monomer' region since quenching pyrene-nucleobase interactions are minimized, ii) low I_{III}/I_I vibronic band ratios due to the high groove polarity, and iii) reduced duplex thermostability, presumably due to perturbations in the duplex hydration spine. In contrast, intercalating pyrenes generally result in: i) weak emission, ii) high I_{III}/I_I-ratios, and iii) increased duplex thermostability, all of which are consequences of pyrene-nucleobase stacking and/or duplex core hydrophobicity. Moreover, π-stacking pyrene dimers display broad and featureless excimer fluorescence at ~490 nm provided that interplanar distances are less than 4 Å.[13]

Hybridization probes are an important subclass of fluorophore-modified oligonucleotides.[14] Pyrene-based hybridization probes[10,15–27] are typically designed to display: i) weak fluorescence in the absence of targets by promoting nucleobase-mediated quenching of the

*Corresponding author: Tel: (+1) 208 885 0108. Fax: (+1) 208 885 6173. hrdlicka@uidaho.edu.

Electronic supplementary information (ESI) available: Protocols for synthesis, purification and quality control of modified ONs, and for thermal denaturation, absorbance and fluorescence studies; MS-data for modified ONs; representative thermal denaturation curves; additional data and discussion concerning thermal denaturation, fluorescence and absorption studies.

pyrene moiety, and ii) increased monomer emission upon target binding by directing the pyrene moiety into a less quenching microenvironment. Base-discriminating probes share the characteristics of hybridization probes and, additionally, display emission intensities that depend on the nucleotide adjacent to the reporter group.[28,29] Most pyrene-based base-discriminating probes[23,30–34] rely on the following principle - the pyrene moiety is i) positioned in a non-quenching groove upon hybridization with complementary targets, while ii) intercalating upon hybridization with mismatched targets, leading to nucleobase-induced quenching of fluorescence.[30,34] Unlike hybridization probes, base-discriminating probes discriminate between complementary and mismatched targets at non-stringent conditions, i.e., at conditions where mismatched duplexes are formed. These probes are therefore well-suited to discriminate SNPs, which are the most frequently occurring genetic variation in the human genome and important biomedical markers.[5]

RNA strands modified with 2'-*O*-(pyren-1-yl)methyluridine monomer **Y** (Fig. 1) are a particularly interesting class of pyrene-based hybridization probes.[16] Their emission intensity increases up to 30-fold upon hybridization with RNA targets, leading to the formation of moderately fluorescent RNA duplexes (quantum yields up to ~25%). Moreover, excellent fluorescent discrimination of mismatched targets is observed. Regrettably, **Y**-modified DNA probes, which are considerably easier to make via machine-assisted solid-phase synthesis than the corresponding RNA probes, exhibit much less consistent changes in fluorescence upon target binding.[15,16] The disparity in fluorescence characteristics is the result of different pyrene binding modes; NMR studies on RNA:RNA and DNA:DNA duplexes modified with a single **Y** monomer have shown that the pyrene moiety predominantly is located in the minor groove and duplex core, respectively.[35]

Glowing locked nucleic acids (LNAs), i.e., DNA, RNA or 2'-*O*-methyl RNA strands modified with two or more non-sequential incorporations of 2'-*N*-(pyren-1-yl)carbonyl-2'-amino-LNA thymine monomer (Fig. 1), are another interesting class of pyrene-based hybridization probes.[19,24,36] Glowing LNA display large increases in fluorescence intensity upon binding to DNA and RNA targets (typically between 2- and 10-fold) and result in the formation of highly thermostable and brightly fluorescent duplexes (quantum yields between 28–99%). This, along with results from molecular modelling studies, suggests that the short rigid linker and bicyclic skeleton of this monomer (locked in a *North*-type conformation) force the pyrene moiety into the minor groove upon duplex formation.[19] However, despite recent improvements in the synthesis of 2'-amino-LNA intermediates,[37] the route to these interesting building blocks still entails approximately twenty steps.[38,39] Development of synthetically more readily available phenomenological mimics of Glowing LNA and **Y**-modified RNA probes is therefore desirable.

Conventional LNA monomers[40–42] (Fig. 1) are known to influence the sugar conformation of neighbouring 2'-deoxyribonucleotides toward increased *North*-type character, whereby LNA-modified duplexes attain more RNA-like geometries.[43,44] This prompted us to hypothesize that DNA-based probes with segments of alternating LNA and 2'-*O*-(pyren-1-yl)methyluridine monomers will display emission characteristics that resemble those of **Y**-modified RNA probes or Glowing LNA, anticipating that LNA-induced tuning of flanking **Y** monomers' furanose conformations from *South*- to *North*-type will position the reporter group in the minor groove upon duplex formation. A similar strategy has been used to modulate the properties of oligodeoxyribonucleotides (ONs) modified with N2'-functionalized 2'-aminouridines[45,46] or 1-(phenylethynyl)pyrene-functionalized 2'-arabinonucleotides,[47] albeit it with partial success.

In this article, thermal denaturation, fluorescence emission and absorption studies on DNA-based probes with segments of alternating LNA and 2'-*O*-(pyren-1-yl)methyluridine

monomers are reported. These probes are relatively straightforward to synthesize; LNA phosphoramidites are commercially available, the corresponding phosphoramidite of monomer **Y** is available in four steps from uridine,[48,49] and machine-assisted solid-phase DNA synthesis is a routine technique. We demonstrate that DNA strands with central L**Y**L**Y**L motifs, unlike their "LNA-free" controls, display large and mismatch-sensitive increases in fluorescence emission upon RNA hybridization due to LNA-induced positional control of the reporter group.

Results and Discussion

Initial studies – identification of probe architecture

To test our hypothesis, we first designed a small set of 9-mer ONs with variable levels of alternating LNA and **Y** monomers in the central region, i.e., L**Y**L, **Y**L**Y** and L**Y**L**Y**L motifs, where 'L' denotes an LNA monomer (**c**-series, Table 1). Following standard machine-assisted synthesis, purification, and quality control of these ONs (see ESI†), thermal denaturation temperatures (T_m's) of the corresponding duplexes with complementary DNA/RNA were determined and compared to reference duplexes involving ONs that are unmodified, only LNA-modified (**a**-series), or only **Y**-modified (**b**-series). As previously reported,[40–42,49] LNA-modified ONs display particularly high thermal affinity toward RNA targets (ΔT_m/modification 7–10 °C, **a**-series, Table 1), while **Y**-modified ONs display very high affinity toward DNA targets (ΔT_m/modification 8–13 °C, **b**-series, Table 1). Interestingly, incorporation of alternating LNA and **Y** monomers significantly reduces the stabilizing effect of either monomer (compare ΔT_m values for **a**- and **b**-series relative to **c**-series, Table 1), presumably due to the opposing mechanisms leading to thermostabilization; LNA monomers induce an increasingly compact and thermostable RNA-like duplex geometry,[43,44] while **Y**-monomers stabilize DNA duplexes through pyrene intercalation,[35] a process that prefers the less compact geometry of *B*-type DNA.[50] Similar observations have been made for duplexes between DNA targets and ONs modified with alternating LNA and 2'-*N*-pyren-1-yl-2'-*N*-methylaminouridine monomers.[45]

Steady-state fluorescence emission spectra of single-stranded probes and the corresponding duplexes with DNA/RNA targets were recorded in thermal denaturation buffer using an excitation wavelength of 350 nm. Single-stranded **Y**-modified reference probe **ON1b** (B**Y**B motif, where 'B' denotes a DNA monomer) displays vibronic peaks at ~376 and ~390 nm and a weak shoulder at ~420 nm (Fig. 2). Binding to DNA/RNA targets results in ~80% decrease in fluorescence intensity. **ON2b** (**Y**B**Y** motif) displays similar characteristics except that weak excimer emission at ~490 nm also is observed. Substitution of the central DNA nucleotide with an LNA monomer only has minor impact on emission characteristics (compare **ON2b** and **ON2c**, Fig. 2).

In contrast, duplex formation between **ON1c**, where monomer **Y** is flanked by two LNA monomers, and DNA/RNA targets, results in moderately increased emission (~1.9-fold and ~4.5-fold increase, as measured at λ_{em} = 376 nm, Fig. 2). Single-stranded **ON3c**, featuring an extended repeat of this motif (L**Y**L**Y**L), displays intense excimer emission but only minimal monomer emission in the region between 370–410 nm. Hybridization with DNA/RNA targets reduces excimer emission by ~75%. Binding to RNA, moreover, results in an extraordinary ~87-fold increase in monomer emission (Fig. 2). Clearly, LNA monomers influence the properties of monomer **Y** in single-stranded **ON3c** and the corresponding duplexes with RNA.

Hybridization-induced excimer-to-monomer emission changes have been previously observed with RNA probes carrying multiple incorporations of 2'-*O*-(pyren-1-

yl)methyladenosine,[22] indicating that this mechanism may be general for RNA-like probes carrying two or more 2'-*O*-(pyren-1-yl)methylribonucleotides.

Extended studies in 9-mer ON context – influence of nucleobases

Encouraged by the large increases in monomer emission upon RNA binding, we set out to examine ONs with central L**Y**L**Y**L motifs in greater detail. Additional 9-mer ONs were synthesized in which the nature of the central nucleotide was systematically varied (**ON4–ON6**, Table 2) as it is known that nucleobases quench pyrene fluorescence with different efficiency – guanine and cytosine are normally the strongest quenchers.[11,51]

In accordance with our initial results, **ON4c–ON6c** display considerably lower affinity toward DNA/RNA targets than would be expected if the stabilizing contributions of LNA and **Y**-monomers were additive (compare ΔT_m values for **ON3–ON6 a**- and **b**-series vs. **c**-series, Tables 1 & 2).[52]

The central DNA nucleotide has only a minor impact on the fluorescence characteristics of **Y**-modified reference ONs and the resulting duplexes with DNA/RNA targets (compare **ON3b–ON6b**, Figs. 2 & S2[†]). Hybridization with DNA/RNA targets generally results in decreased monomer emission (Fig. 3).

In contrast, the nature of the central LNA nucleotide greatly influences the excimer emission of single-stranded L**Y**L**Y**L probes, which decreases in the order L: **a** ~ **t** > **c** > **g** (compare **ON3c–ON6c**-series, Figs. 2 & S2[†]). Large increases in monomer emission are observed upon RNA binding, while DNA binding results in more subtle increases (19–118 fold vs 3.8–69 fold, respectively, Fig. 3).[52] In fact, the increases in emission intensity upon RNA binding are greater than those reported for **Y**-modified RNA, Glowing LNA, and other pyrene-based hybridization or base-discriminating probes.[15–27,30–34,53]

The results demonstrate that i) LNA monomers have a substantial influence on the photophysical properties (and hence position) of the pyrene moieties of flanking **Y** monomers, both in single-stranded probes and duplexes, and ii) emission intensities of duplexes with RNA targets are largely unaffected by the nature of the central LNA nucleotide (compare emission intensity of **ON3c–ON6c** vs RNA, Fig. 3), which hints at weak pyrene-nucleobase interactions.

Rationalization of emission trends via absorption spectroscopy

Absorbance spectra of **ON1–ON6** and the corresponding duplexes with DNA/RNA targets were recorded to rationalize the observed emission trends (Figs. S3 & S4[†]). **Y**-modified reference probes (**b**-series) display bathochromic shifts of pyrene absorption maxima upon hybridization with DNA/RNA targets ($\Delta\lambda$ = 0–4 nm, Table 3), which is consistent with pyrene intercalation[54] and the observed hybridization-induced decreases in emission intensity (Fig. 3).

With the exception of **ON4c**, bathochromic shifts were also observed upon DNA binding of **ON1c–ON6c** (Table 3), which explains the moderate fluorescence intensity of these duplexes (Fig. 3). With the exception of **ON2c**, RNA binding of **ON1c–ON6c** results in hypsochromic and hyperchromic shifts ($\Delta\lambda$ from −6 to −2 nm, Table 3), which is consistent with hybridization-induced pyrene-nucleobase destacking[54] and increased fluorescence emission (Fig. 3). The low I_{III}/I_I vibronic band ratio observed for duplexes between these probes and RNA, further suggests that the pyrene moieties are localized in the polar minor groove (Figs. 2 & S2[†]).[12]

As mentioned, two exceptions to these general trends are observed: i) **ON2c** displays bathochromic shifts of pyrene absorption maxima upon DNA as well as RNA binding (Table 3), which is in agreement with intercalation and the observed hybridization-induced decreases in fluorescence emission (Fig. 3), and ii) **ON4c** displays a slight hypsochromic shift upon DNA binding (Table 3), which is consistent with the hybridization-induced increases in monomer emission (Fig. 3).

The results demonstrate that the high LNA density of the L**Y**L**Y**L motif changes the preferred pyrene binding mode of monomer **Y** from intercalation to increasing groove localization. This renders the L**Y**L**Y**L motif as a promising element in the design of RNA hybridization probes.

Generality of LYLYL-probes – studies in 13-mer sequence contexts

To examine the generality of this probe architecture, four 13-mer ONs featuring the L**Y**L**Y**L motif were prepared, in which the nature of the central LNA monomer again was systematically varied (**ON7–ON10**, Table 4). Briefly, thermal denaturation experiments demonstrate that these probes – as compared to unmodified reference strands – display: i) lower affinity toward DNA targets (Table S3[†]), ii) slightly higher thermal affinity toward complementary RNA (compare T_m's for **ON7–ON10** vs **ON7ref–ON10ref**, Table 4), and iii) less efficient thermal discrimination of centrally mismatched RNA targets (compare ΔT_m's, Table 4).

ON7–ON10 display similar spectral characteristics as the 9-mer series, i.e., i) very large increases in pyrene monomer emission upon hybridization with RNA targets but more subtle increases with DNA targets (21–83 fold vs 1.4–10 fold, respectively, Figs. 4 & S7[†]), and ii) significant hypsochromic and hyperchromic shifts of pyrene absorption maxima upon hybridization with RNA targets ($\Delta\lambda$ from −7 to −6 nm, Table 5; for spectra, see Fig. S9[†]), but bathochromic shifts upon DNA binding (Table S4[†]). The nature of the central LNA nucleotide is again found only to have relatively minor impact on the emission intensity of the resulting duplexes with complementary RNA (compare intensity of **ON7–ON10** vs RNA, Fig. 4).

Fluorescence-based SNP discrimination

Interestingly, **ON7–ON10** display excellent fluorescent discrimination of centrally mismatched RNA targets as the resulting duplexes exhibit much lower monomer emission than fully complementary duplexes (Figs. S6 & S8[†]). Large mismatch discrimination factors – defined as the intensity ratio between matched and mismatched duplexes – of between 2.1 and 19 are observed (Fig. 4). Consistent with these results, duplex formation with mismatched RNA targets is associated with less pronounced hypsochromic and hyperchromic shifts of pyrene absorption peaks than with complementary RNA targets (Table 5 and Fig S9[†]). This strongly suggests that the pyrene moieties of **ON7–ON10** intercalate more readily into mismatched duplexes, leading to nucleobase-mediated quenching of fluorescence.

Thus, DNA probes with central L**Y**L**Y**L-motifs are base-discriminating probes that can discriminate between complementary and mismatched targets at non-stringent conditions, i.e., conditions where mismatched duplexes are formed (Fig. 5). These properties render the title probes as promising SNP-discriminating RNA detection probes.

Conclusions

LNA monomers significantly influence the photophysical properties of flanking 2'-*O*-(pyren-1-yl)methyluridine **Y** monomers both in single-stranded probes and duplexes. Specifically, DNA strands with central L**Y**L**Y**L motifs display between 19- to 119-fold increases in emission intensity upon RNA binding, while corresponding "LNA-free" probes only result in 0.4- to 1.6-fold intensity changes. Although LNA-induced positional tuning of flanking reporter groups has been previously pursued,[45–47] the current study represents the first example where this strategy has resulted in such dramatic and general changes in probe/duplex properties. The observed RNA-induced intensity increases for the L**Y**L**Y**L probes are up to an order of magnitude greater than for the synthetically more complex Glowing LNA,[19,24,36] **Y**-modified RNA,[16,22] or other pyrene-based hybridization probes.[15,17,18,20,21,23,25–27] Moreover, the probes display excellent fluorescent discrimination of centrally mismatched RNA targets under non-stringent conditions (discrimination factors between 2.1 and 19). The above characteristics were observed in all eight probes containing the L**Y**L**Y**L motif, underscoring the robustness of this motif as a component of SNP-discriminating RNA detection probes.

Considerable efforts have been devoted in recent years to the design, synthesis and characterization of elaborate nucleotide monomers in the search of building blocks that confer new function to nucleic acids. The current study demonstrates that a combination of existing and synthetically more readily (or even commercially) available building blocks can result in oligonucleotides-based probes with unprecedented photophysical properties. Given the plethora of chemically modified nucleotide monomers developed for therapeutic,[55–58] diagnostic,[1,10,28,29,59] and other applications,[60–63] it is highly probable that other combinations of structure-tuning and fluorophore-functionalized monomers will be identified for applications in nucleic acid diagnostics. Studies along these lines are ongoing in our laboratory.

Supplementary Material

Refer to Web version on PubMed Central for supplementary material.

Acknowledgments

We thank Dr. Lee Deobald (EBI Murdock Mass Spectrometry Center) for assistance with mass spectrometric analyses. Initial contributions by Sanne Andersen (Univ. Southern Denmark and Univ. Idaho) are appreciated.

Funding. We appreciate financial support from award number R01 GM088697 from the National Institute of General Medical Sciences, National Institutes of Health, Idaho NSF EPSCoR and the Student Grant Program at University of Idaho (U80203).

Notes and References

1. Asseline U. Curr. Org. Chem. 2006; 10:491–518.
2. Juskowiak B. Anal. Bioanal. Chem. 2011; 399:3157–3176. [PubMed: 21046088]
3. Vet JA, Majithia AR, Marras SA, Tyagi S, Dube S, Poiesz BJ, Kramer FR. Proc Natl Acad Sci. USA. 1999; 96:6394–6399. [PubMed: 10339598]
4. Wilhelm J, Pingoud A. Chem Bio Chem. 2003; 4:1120–1128.
5. Kim S, Misra A. Annu. Rev. Biomed. 2007; 9:289–320.
6. Levsky JM, Singer RH. J. Cell Sci. 2003; 116:2833–2838. [PubMed: 12808017]
7. Armitage BA. Curr. Opin. Chem. Biol. 2011; 15:806–812. [PubMed: 22055496]
8. Tyagi S. Nat Methods. 2009; 6:331–338. [PubMed: 19404252]
9. Malinovskii VL, Wenger D, Häner R. Chem. Soc. Rev. 2010; 39:410–422. [PubMed: 20111767]

10. Østergaard ME, Hrdlicka PJ. Chem. Soc. Rev. 2011; 40:5771–5788. [PubMed: 21487621]
11. Manoharan M, Tivel KL, Zhao M, Nafisi K, Netzel TL. J. Phys. Chem. 1995; 99:17461–17472.
12. Kalyanasundaram K, Thomas JK. J. Am. Chem. Soc. 1977; 99:2039–2044.
13. Winnik FM. Chem. Rev. 1993; 93:587–614.
14. Seitz, O.; Schmuck, EC.; Wennemers, H. Highlights in Bioorganic Chemistry. Wiley-VCH Verlag GmbH & Co.; 2004. Homogeneous DNA Detection; p. 311-328.
15. Yamana K, Iwase R, Furutani S, Tsuchida H, Zako H, Yamaoka T, Murakami A. Nucleic Acids Res. 1999; 27:2387–2392. [PubMed: 10325429]
16. Yamana K, Zako H, Asazuma K, Iwase R, Nakano H, Murakami A. Angew. Chem. Int. Ed. 2001; 40:1104–1106.
17. Mahara A, Iwase R, Sakamoto T, Yamana K, Yamaoka T, Murakami A. Angew. Chem. Int. Ed. 2002; 41:3648–3650.
18. Korshun VA, Stetsenko DA, Gait MJ. J. Chem. Soc. Perkin Trans. 1. 2002; 41:1092–1104.
19. Hrdlicka PJ, Babu BR, Sørensen MD, Harrit N, Wengel J. J. Am. Chem. Soc. 2005; 127:13293–13299. [PubMed: 16173760]
20. Astakhova IV, Korshun VA, Wengel J. Chem. Eur. J. 2008; 14:11010–11026. [PubMed: 18979465]
21. Honcharenko D, Zho C, Chattopadhyaya J. J. Org. Chem. 2008; 73:2829–2842. [PubMed: 18331060]
22. Wang G, Bobkov GV, Mikhailov SN, Schepers G, Van Aerschot A, Rozenski J, van der Auweraer M, Herdewijn P, Feyter SD. Chem Bio Chem. 2009; 10:1175–1185.
23. Østergaard ME, Guenther DC, Kumar P, Baral B, Deobald L, Paszczynski AJ, Sharma PK, Hrdlicka PJ. Chem. Commun. 2010:4929–4931.
24. Østergaard ME, Cheguru P, Papasani MR, Hill RA, Hrdlicka PJ. J. Am. Chem. Soc. 2010; 132:14221–14228. [PubMed: 20845923]
25. Astakhova IV, Lindegaard D, Korshun VA, Wengel J. Chem. Commun. 2010; 46:8362–8364.
26. Förster U, Lommel K, Sauter D, Grünewald C, Engels JW, Wachtveitl J. Chem Bio Chem. 2010; 11:664–672.
27. Mansawat W, Boonlua C, Siriwong K, Vilaivan T. Tetrahedron. 2012; 68:3988–3995.
28. Okamoto A, Saito Y, Saito I. J. Photochem. Photobiol. C. 2005; 6:108–122.
29. Dodd DW, Hudson RHE. Mini-Rev. Org. Chem. 2009; 6:378–391.
30. Okamoto A, Kanatani K, Saito I. J. Am. Chem. Soc. 2004; 126:4820–4827. [PubMed: 15080686]
31. Hwang GT, Seo YJ, Kim SJ, Kim BH. Tetrahedron Lett. 2004; 45:3543–3546.
32. Saito Y, Hanawa K, Motegi K, Omoto K, Okamoto A, Saito I. Tetrahedron Lett. 2005; 46:7605–7608.
33. Dohno C, Saito I. Chem Bio Chem. 2005; 6:1075–1081.
34. Østergaard ME, Kumar P, Baral B, Guenther DC, Anderson BA, Ytreberg FM, Deobald L, Paszczynski AJ, Sharma PK, Hrdlicka PJ. Chem. Eur. J. 2011; 17:3157–3165. [PubMed: 21328492]
35. Nakamura M, Fukunaga Y, Sasa K, Ohtoshi Y, Kanaori K, Hayashi H, Nakano H, Yamana K. Nucleic Acids Res. 2005; 33:5887–5895. [PubMed: 16237124]
36. Østergaard ME, Maiti J, Babu BR, Wengel J, Hrdlicka PJ. Bioorg. Med. Chem. Lett. 2010; 20:7265–7268. [PubMed: 21071224]
37. Madsen AS, Jørgensen AS, Jensen TB, Wengel J. J. Org. Chem. 2012; 77:10718–10728. [PubMed: 23145501]
38. Sørensen MD, Petersen M, Wengel J. Chem. Commun. 2003:2130–2131.
39. Rosenbohm C, Christensen SM, Sørensen MD, Pedersen DS, Larsen LE, Wengel J, Koch T. Org. Biomol. Chem. 2003; 1:655–663. [PubMed: 12929452]
40. Koshkin AA, Singh SK, Nielsen P, Rajwanshi VK, Kumar R, Meldgaard M, Olsen CE, Wengel J. Tetrahedron. 1998; 54:3607–3630.
41. Obika S, Nanbu D, Hari Y, Andoh JI, Morio KI, Doi T, Imanishi T. Tetrahedron Lett. 1998; 39:5401–5404.

42. Kaur H, Babu BR, Maiti S. Chem. Rev. 2007; 107:4672–4697. [PubMed: 17944519]
43. Petersen M, Nielsen CB, Nielsen KE, Jensen GA, Bondensgaard K, Singh SK, Rajwanshi VK, Koshkin AA, Dahl BM, Wengel J, Jacobsen JP. J. Mol. Recognit. 2000; 13:44–53. [PubMed: 10679896]
44. Petersen M, Bondensgaard K, Wengel J, Jacobsen JP. J. Am. Chem. Soc. 2002; 124:5974–5982. [PubMed: 12022830]
45. Kalra N, Babu BR, Parmar VS, Wengel J. Org. Biomol. Chem. 2004; 2:2885–2887. [PubMed: 15480448]
46. Kalra N, Parlato MC, Parmar VS, Wengel J. Bioorg. Med. Chem. Lett. 2006; 16:3166–3169. [PubMed: 16621554]
47. Astakhova IV, Ustinov AV, Korshun VA, Wengel J. Bioconjugate Chem. 2011; 22:533–539.
48. Yamana K, Ohashi Y, Nunota K, Kitamura M, Nakano H, Sangen OS. Tetrahedron Lett. 1991; 32:6347–6350.
49. Karmakar S, Anderson BA, Rathje RL, Andersen S, Jensen T, Nielsen P, Hrdlicka PJ. J. Org. Chem. 2011; 76:7119–7131. [PubMed: 21827174]
50. Marin V, Hansen HF, Koch TR, Armitage BA. J. Biomol. Struc. Dyn. 2004; 21:841–850.
51. Seo YJ, Ryu JH, Kim BH. Org. Lett. 2005; 7:4931–4933. [PubMed: 16235925]
52. For a discussion regarding T_m's of reference duplexes as well as duplexes between **ON3c–ON6c** and centrally mismatched RNA targets, see ESI†.
53. While quantum yields were not determined in this study, direct comparison with corresponding duplexes involving Glowing LNAs (quantum yields 80–90%)[24] indicates that the duplex between **ON3c** and complementary RNA is approximately half as bright.
54. Asanuma H, Fujii T, Kato T, Kashida H. J. Photochem. Photobiol. C. 2012; 13:124–135.
55. Freier SM, Altmann K-H. Nucleic Acids Res. 1997; 25:4429–4443. [PubMed: 9358149]
56. Watts JK, Deleavey GF, Damha MJ. Drug Disc. Today. 2008; 13:842–855.
57. Duca M, Vekhoff P, Oussedik K, Halby L, Arimondo PB. Nucleic Acids Res. 2008; 36:5123–5138. [PubMed: 18676453]
58. Prakash TP. Chem. Biodiv. 2011; 8:1616–1641.
59. Filichev VV, Pedersen EB. Wiley Encycl. Chem. Biol. 2009; 1:493–524.
60. Amblard F, Cho JH, Schinazi RF. Chem. Rev. 2009; 109:4207–4220. [PubMed: 19737023]
61. Sinkeldam RW, Greco NJ, Tor Y. Chem. Rev. 2010; 110:2579–2619. [PubMed: 20205430]
62. Bandy TJ, Brewer A, Burns JR, Marth G, Nguyen TN, Stulz E. Chem. Soc. Rev. 2011; 40:138–148. [PubMed: 20694258]
63. Loakes D. Organophosphorus Chem. 2012; 41:169–250. and previous volumes in this annual series.

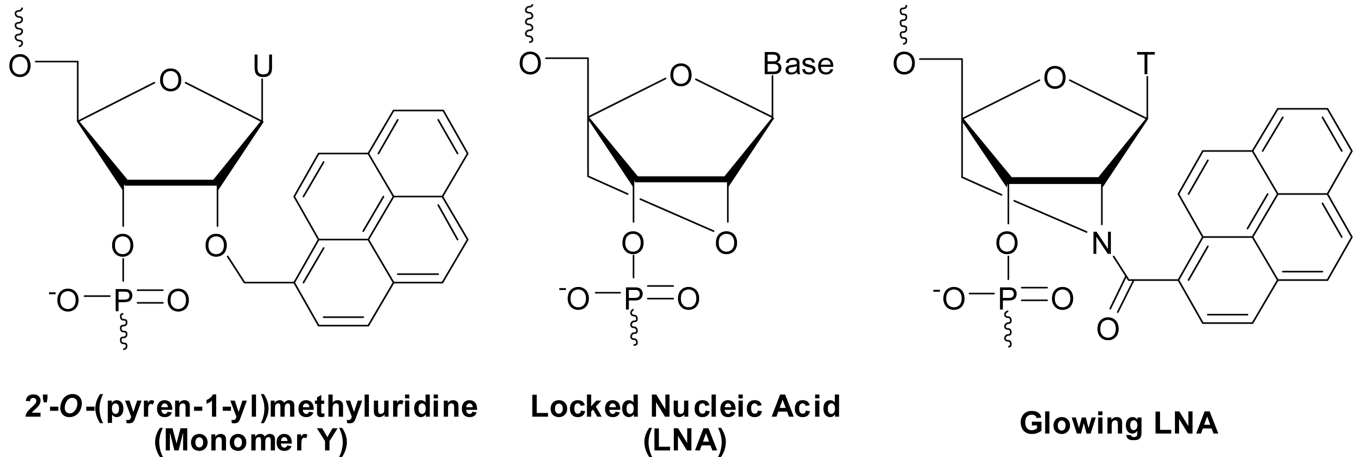

Figure 1.
Structures of 2'-*O*-(pyren-1-yl)methyluridine, conventional LNA, and Glowing LNA monomers.

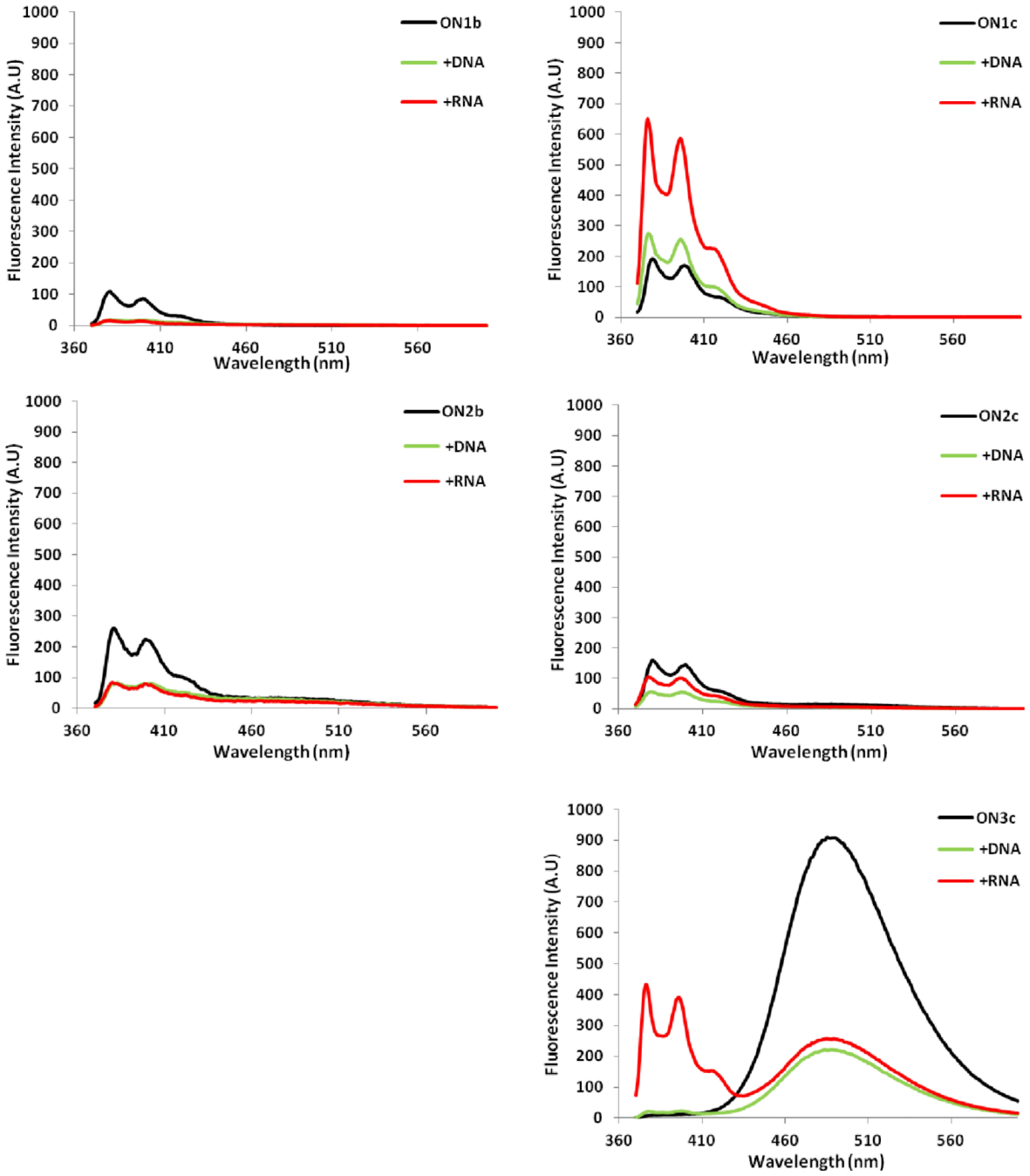

Figure 2.

Steady-state fluorescence emission spectra of **ON1–ON3** and the corresponding duplexes with DNA/RNA targets. Spectra were recorded at T = 5 °C using λ_{ex} = 350 nm and each strand at 1.0 μM concentration in T_m buffer.

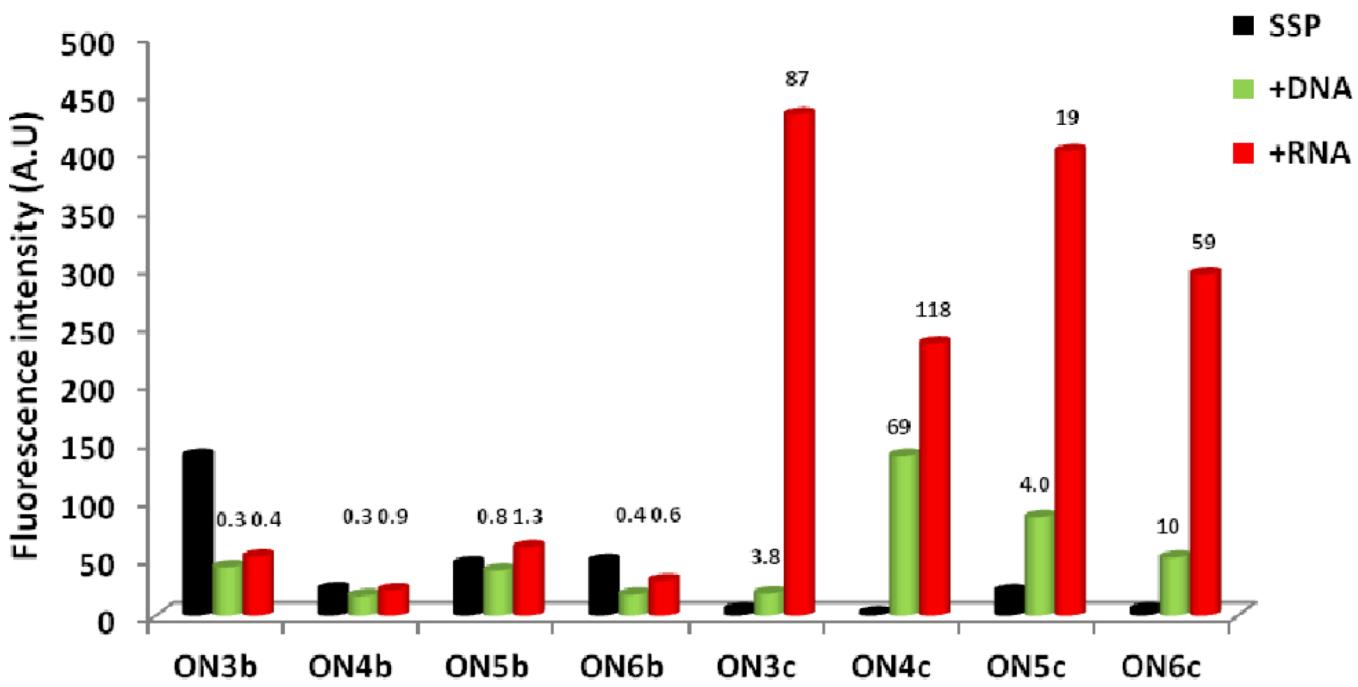

Figure 3.

Fluorescence intensity of **ON3–ON6** and the corresponding duplexes with DNA or RNA targets as measured at λ_{em} = 376 nm. Hybridization-induced increases/decreases – defined as the intensity ratio between a duplex and single-stranded probe (SSP) – are listed above corresponding histograms. Spectra were recorded at T = 5 °C using λ_{ex} = 350 nm and each strand at 1.0 μM concentration in T_m buffer. For spectra, see Figs. 2 & S2†.

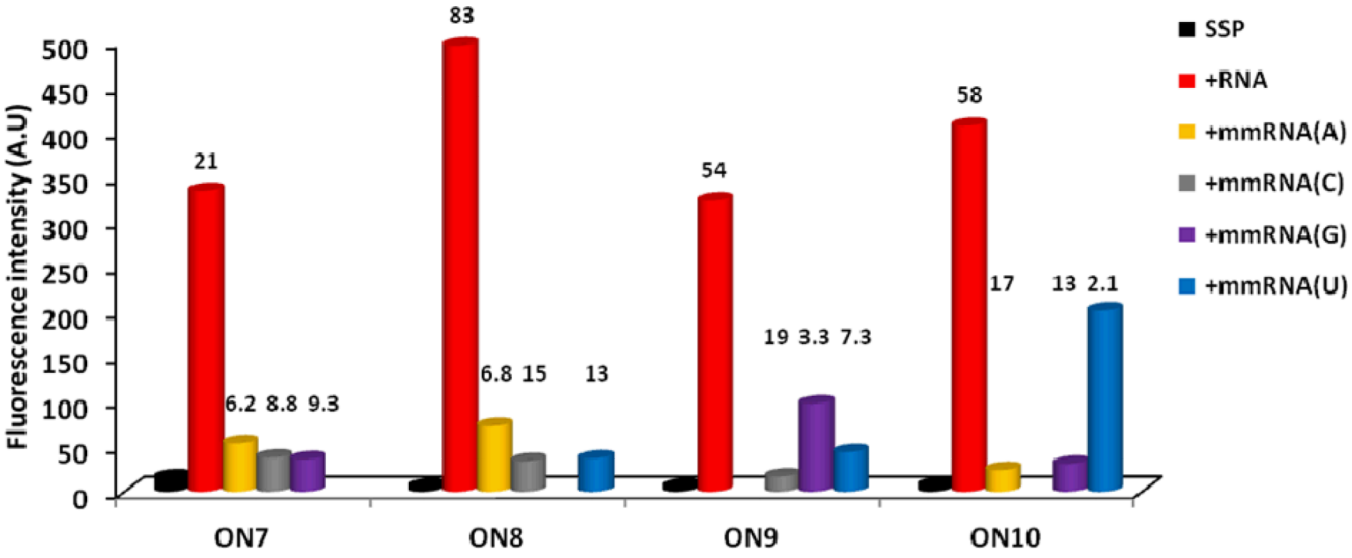

Figure 4.

Fluorescence intensity of single-stranded probes and duplexes with complementary or centrally mismatched RNA targets as measured at λ_{em} = 376 nm (mismatched nucleotide listed in parenthesis). Hybridization-induced increases (defined as the intensity ratio between a matched duplex and single-stranded probe) and discrimination factors (defined as the intensity ratio between a matched and mismatched duplex) are listed above the corresponding histograms. Spectra were recorded at T = 5 °C using λ_{ex} = 350 nm and each strand at 1.0 μM concentration in T_m buffer. For spectra, see Fig S6†.

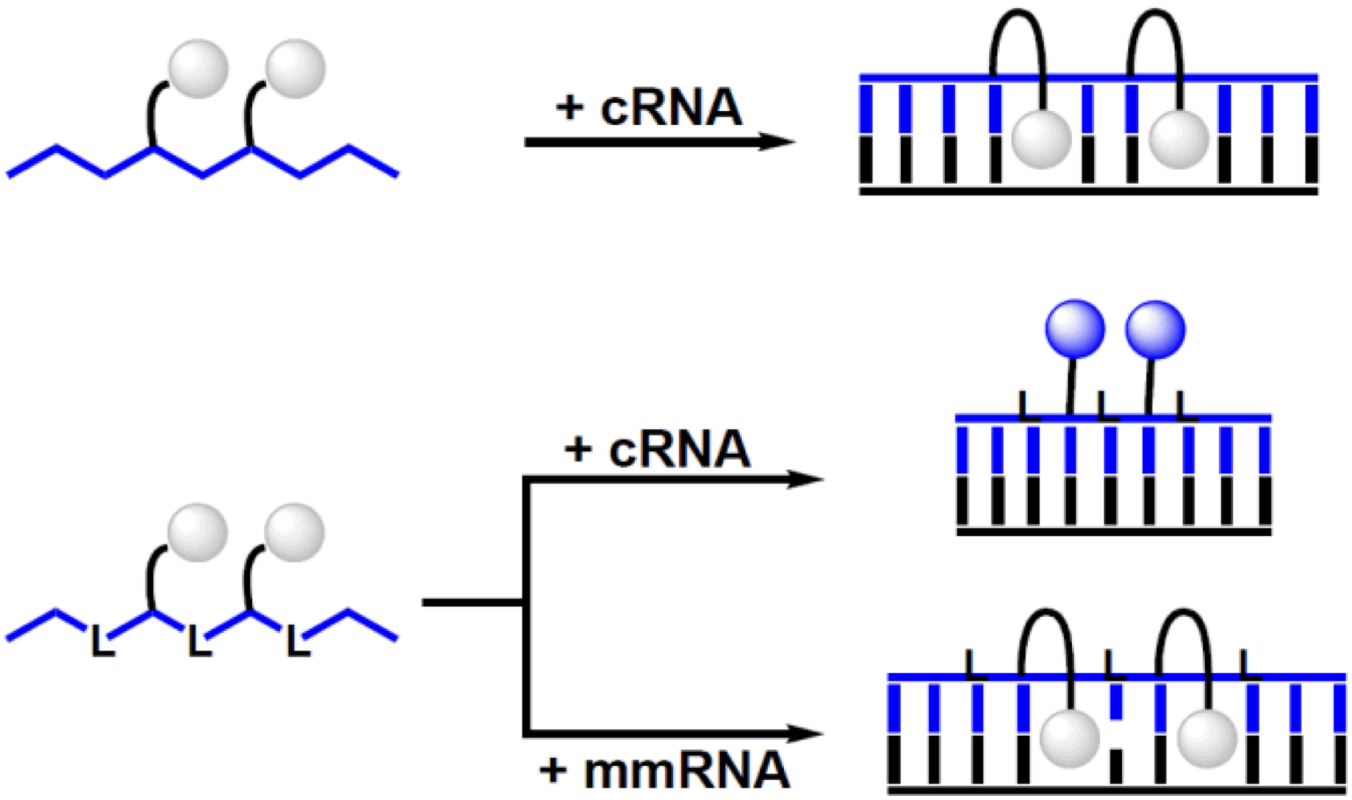

Figure 5.

Principle of SNP-discriminating RNA detection probes reported herein. Upper: **Y**-modified 'LNA-free' reference probes do not result in substantial fluorescence changes upon hybridization with RNA targets due to intercalation of pyrene. Lower: DNA strands with alternating incorporations of LNA and **Y** monomers result in large hybridization-induced increases in emission with complementary RNA (pyrene in minor groove) but not with mismatched targets (intercalation of pyrene). Droplets represent pyrene moiety of monomer **Y**. 'L', 'cRNA' and 'mmRNA' denote conventional LNA monomer, complementary RNA, and centrally mismatched RNA target, respectively.

Table 1

Thermal denaturation temperatures (T_m's) of duplexes between **ON1–ON3** and complementary DNA/RNA targets.[a]

		T_m [ΔT_m]/°C	
ON	**Sequence**	**+DNA**	**+RNA**
ON1a	5'-GTG **a**T**a** TGC	37.0 [+7.5]	41.0 [+14.5]
ON1b	5'-GTG A**Y**A TGC	42.0 [+12.5]	31.0 [+4.5]
ON1c	5'-GTG **a****Y****a** TGC	37.0 [+7.5]	35.0 [+8.5]
ON2a	3'-CAC T**a**T CAC	33.0 [+3.5]	34.0 [+9.5]
ON2b	3'-CAC **Y**A**Y** ACG	46.0 [+16.5]	27.0 [+2.5]
ON2c	3'-CAC **Y****a****Y** ACG	35.0 [+5.5]	21.0 [−3.5]
ON3a	3'-CA**c** T**a**T **a**CG	43.5 [+14.0]	50.5 [+26.0]
ON3c	3'-CA**c** **Y****a****Y** **a**CG	32.5 [+3.0][b]	24.5 [±0.0][b]

[a] T_m's determined as the maximum of the first derivative of thermal denaturation curves (A_{260} vs T) recorded in medium salt buffer ([Na^+] = 110 mM, [Cl^-] = 100 mM, pH 7.0 (NaH_2PO_4/Na_2HPO_4)), using 1.0 μM of each strand. T_m's are averages of at least two measurements within 1.0 °C unless otherwise noted. ΔT_m = change in T_m relative to unmodified reference duplexes, which have the following values (DNA/RNA): 29.5/26.5 °C (**ON1** ref) and 29.5/24.5 °C (**ON2** & **ON3** ref). A = adenin-9-yl DNA monomer, C = cytosin-1-yl DNA monomer, G = guanin-9-yl DNA monomer, T = thymin-1-yl DNA monomer, **a** = adenin-9-yl LNA monomer, **c** = 5-methylcytosin-1-yl LNA monomer, **g** = guanin-9-yl LNA monomer, **t** = thymin-1-yl LNA monomer. For structures of LNA and **Y** monomers, see Fig. 1.

[b] Broad transition (Fig. S1†). Error of T_m value estimated at ±3.0 °C.

Table 2

Thermal denaturation temperatures (T_m's) of duplexes between **ON4–ON6** and complementary DNA/RNA targets.[a]

		T_m [ΔT_m]/°C	
ON	**Sequence**	**+DNA**	**+RNA**
ON4a	3'-CA**c** T**t**T **a**CG	43.5 [+12.5]	50.0 [+21.5]
ON4b	3'-CAC **Y**T**Y** ACG	34.5 [+3.5]	22.5 [−6.0]
ON4c	3'-CA**c** **Y**t**Y** **a**CG	nt	26.5 [−2.0][b]
ON5a	3'-CA**c** T**c**T **a**CG	48.5 [+12.5]	61.0 [+23.5]
ON5b	3'-CAC **Y**C**Y** ACG	39.0 [+3.0]	27.0 [−10.5]
ON5c	3'-CA**c** **Y**c**Y** **a**CG	37.0 [+1.0]	46.5 [+9.0]
ON6a	3'-CA**c** T**g**T **a**CG	50.0 [+13.0]	56.5 [+23.0]
ON6b	3'-CAC **Y**G**Y** ACG	47.0 [+10.0]	29.0 [−4.5]
ON6c	3'-CA**c** **Y**g**Y** **a**CG	31.0 [−6.0]	37.5 [+4.0]

[a]Unmodified reference duplexes display the following T_m's (DNA/RNA): 31.0/28.5 °C (**ON4** ref), 36.0/37.5 °C (**ON5** ref), and 37.0/33.5 °C (**ON6** ref). "nt" denotes no transition. For experimental conditions and definitions, see Table 1.

[b]Broad transition. Error of T_m value estimated at ±3.0 °C.

Table 3

Pyrene absorption maxima for **ON1–ON6** and the corresponding duplexes with DNA and RNA targets.[a]

		λ_{max} [Δλ] (nm)		
ON	**Sequence**	**SSP**	**+DNA**	**+RNA**
ON1b	5'-GTG A**Y**A TGC	348	352 [+4]	352 [+4]
ON2b	3'-CAC **Y**A**Y** ACG	349	352 [+3]	352 [+3]
ON4b	3'-CAC **Y**T**Y** ACG	349	352 [+3]	351 [+2]
ON5b	3'-CAC **Y**C**Y** ACG	349	352 [+3]	350 [+1]
ON6b	3'-CAC **Y**G**Y** ACG	352	352 [±0]	352 [±0]
ON1c	5'-GTG **aYa** TGC	347	351 [+4]	343 [−6]
ON2c	3'-CAC **YaY** ACG	348	352 [+4]	351 [+3]
ON3c	3'-CA**c YaY a**CG	344	351 [+7]	342 [−2]
ON4c	3'-CA**c YtY a**CG	346	345 [−1]	343 [−3]
ON5c	3'-CA**c YcY a**CG	348	352 [+4]	342 [−6]
ON6c	3'-CA**c YgY a**CG	346	352 [+6]	343 [−3]

[a] Δλ = shift in absorption maximum relative to single-stranded probe (SSP). T = 5 °C; each strand used at 1.0 μM concentration in T_m buffer.

Table 4

T_m's of duplexes between **ON7–ON10** and complementary or mismatched RNA.[a]

			T_m [ΔT_m]/°C			
			5'-rCG CA AA**B**AA AC GC			
ON	**Sequences**	**B=**	**A**	**C**	**G**	**U**
ON7	3'-GC GT t**Y**a**Y**t TG CG		44.0 [−6.0]	42.0 [−8.0]	44.0 [−6.0]	**50.0**
ON7 ref	3'-GC GT TTATT TG CG		36.0 [−10.0]	35.0 [−11.0]	39.0 [−7.0]	**46.0**
ON8	3'-GC GT t**Y**c**Y**t TG CG		44.0 [−12.0]	41.5 [−14.5]	**56.0**	44.0 [−12.0]
ON8 ref	3'-GC GT TTCTT TG CG		35.0 [−17.0]	30.0 [−22.0]	**52.0**	33.0 [−19.0]
ON9	3'-GC GT t**Y**t**Y**t TG CG		**50.0**	45.0 [−5.0]	44.5 [−5.5]	46.0 [-4.0]
ON9 ref	3'-GC GT TTTTT TG CG		**47.0**	33.0 [−14.0]	43.0 [−4.0]	36.0 [−11.0]
ON10	3'-GC GT t**Y**g**Y**t TG CG		44.0 [−10.0]	**54.0**	44.5 [−9.5]	44.5 [−9.5]
ON10 ref	3'-GC GT TTGTT TG CG		35.0 [−16.0]	**51.0**	39.0 [−12.0]	39.0 [−12.0]

[a]For conditions of thermal denaturation experiments, see Table 1. T_m's of fully matched duplexes are shown in bold. ΔT_m = change in T_m relative to fully matched duplex.

Table 5

Pyrene absorption maxima for **ON7–ON10** and the corresponding duplexes with matched/mismatched RNA targets.[a]

		λ_{max} [Δλ] (nm)				
Probe	**Sequence**	**SSP**	**+RNA (A)**	**+RNA (C)**	**+RNA (G)**	**+RNA (U)**
ON7	3'-GC GT **t<u>Y</u>a<u>Y</u>t** TG CG	348	346 [−2]	346 [−2]	344 [−4]	**342 [−6]**
ON8	3'-GC GT **t<u>Y</u>c<u>Y</u>t** TG CG	348	345 [−3]	344 [−4]	**342 [−6]**	347 [−1]
ON9	3'-GC GT **t<u>Y</u>t<u>Y</u>t** TG CG	348	**342 [−6]**	349 [+1]	349 [+1]	345 [−3]
ON10	3'-GC GT **t<u>Y</u>g<u>Y</u>t** TG CG	349	346 [−3]	**342 [−7]**	346 [−3]	343 [−6]

[a]Conditions as described in footnote of Table 1. Absorption maxima for matched duplexes are shown in bold. Spectra recorded at T = 5 °C using each strand at 1.0 μM concentration in T_m buffer. SSP denotes single-stranded probe. For spectra, see Fig. S9†.